

Åshild Fredriksen¹, Giulio Tribulato^{1,2}, Christopher Watts³, and Claudia Riccardi²

¹Department of Physics and Technology, University of Tromsø, N-9037 Tromsø, Norway

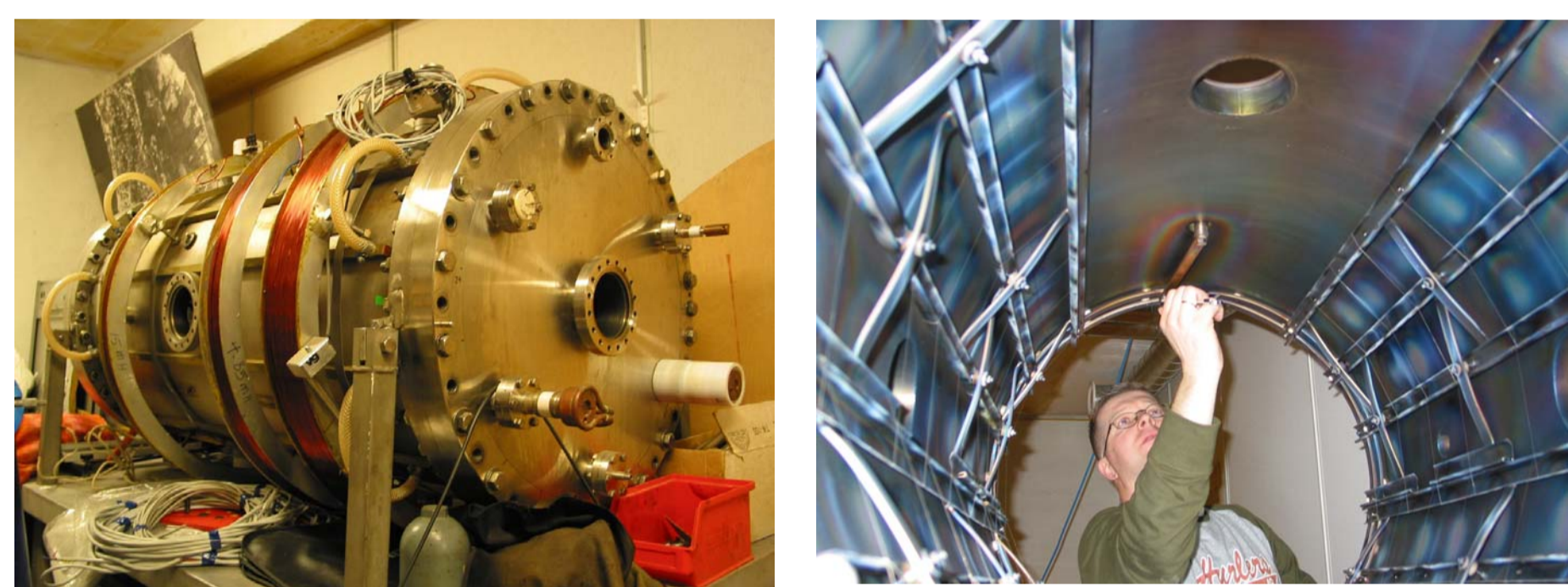
²Dep. Physics, University of Milano-Bicocca, Italy, ³Dep. of Electrical and Computer Engineering, University of New Mexico, Albuquerque.

Introduction

The Njord^{*)} device at AuroLab, University of Tromsø, has been constructed to carry out experiments on instabilities and heating in plasma flows and beams, with relevance to near-Earth space plasmas. For plasma production, Njord combines a 13.56 MHz RF source with a Double Plasma chamber equipped with filaments along the walls. The source is equipped with two coils operated at 0-6A, providing magnetic field of up to 150 G. A third coil (the guide coil) is operated at 0-40 A, to increase plasma density in the main chamber. The first RF plasmas were produced October 2006. For the initial characterization of the plasma, a RF-compensated probe was constructed and tested, and measurements were compared with results from a double probe system. Plasmas have been produced applying RF power from 300-900 W, and at pressures from 3×10^{-4} — 1×10^{-3} mbar. Axial profiles of density, temperature and plasma potential were obtained down-stream from the middle of the source for a distance of 23 cm, and radial profiles were obtained 15 cm downstream from the edge of the source. In the present poster, we report the construction of the device and the results from the first measurements.

*) In Norse mythology, Njord is the god of wind, fertile land along the coast, as well as seamanship, sailing and fishing. The prose Edda says he has the power to calm the sea or fire (Wikipedia).

The construction of the device



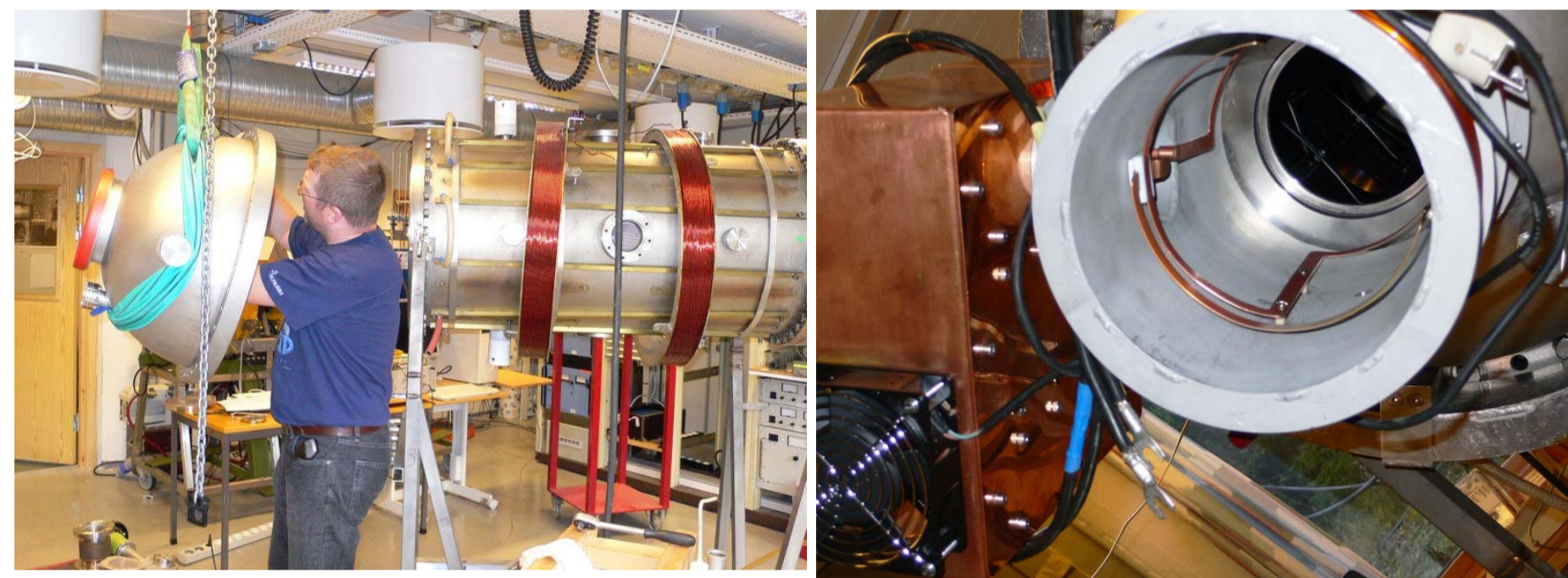
Starting point, an old DP chamber

Mounting filament rack inside chamber



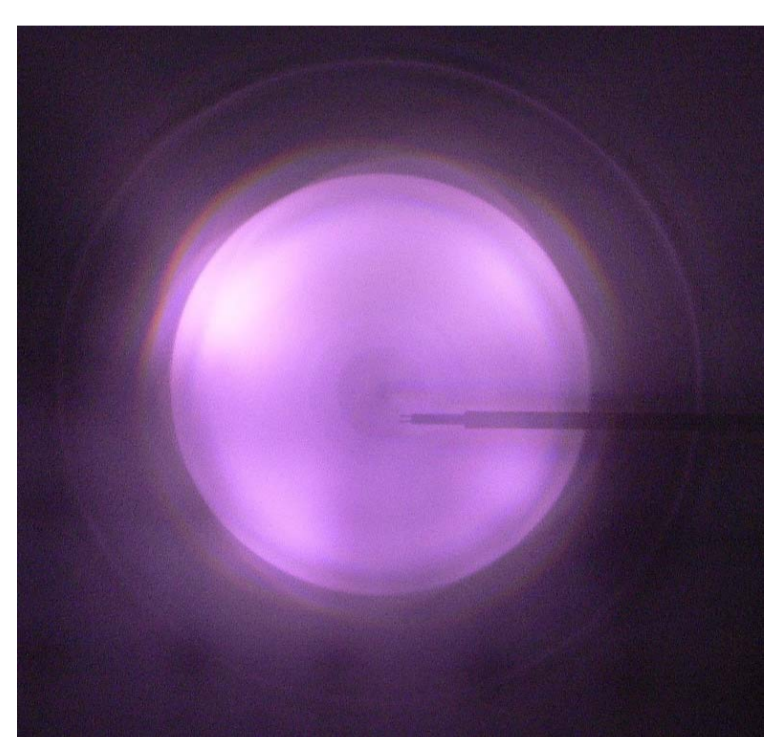
Anode chamber w/grid ready to mount.

Inserting anode chamber

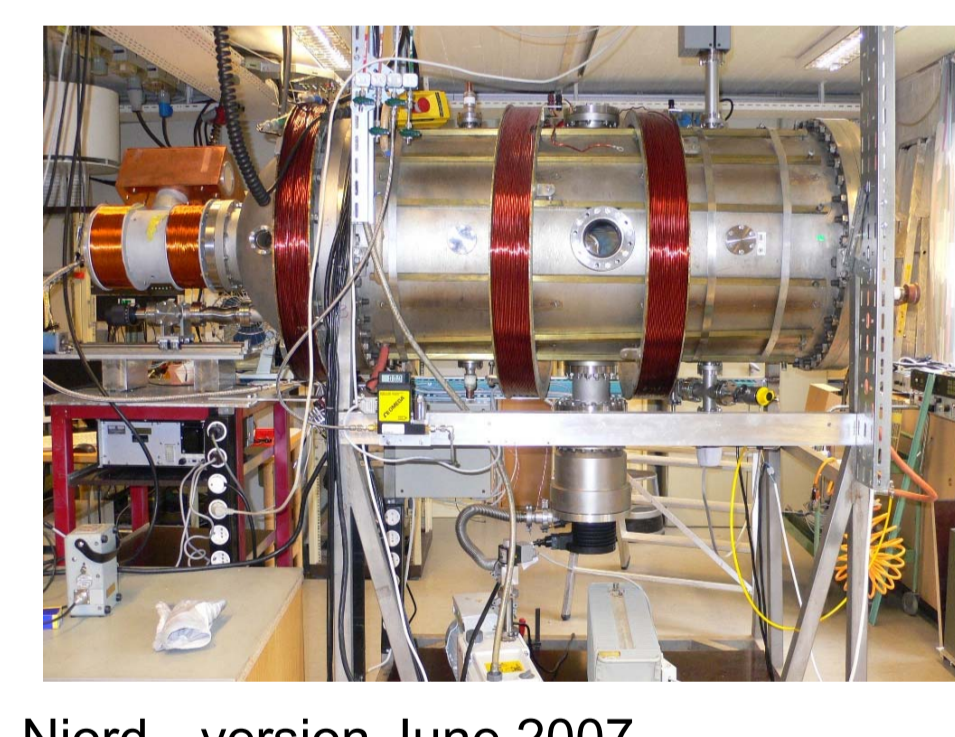


Mounting dome for antenna system

Antenna system mounted and ready for pyrex tube and closing



First plasma October 2006.



Njord—version June 2007

Chamber specifications

Total length: 1.20m (cylinder) + 0.30m (dome) = 1.5m Radius: 60 cm.
Ports: 1x CF200mm and 4x CF40mm on dome (1 axial, 3 radial)+ 5x CF100mm (1 axial, 4 radial) and 14x CF40mm (8 radial, 6 axial) on main chamber.
At the end opposite to the dome an anode cage of length 30 cm is inserted inside and electrically insulated from the main chamber. In front of the anode cage facing the main chamber is an electrically insulated plate with a meshed, D15 cm hole in the middle, which can be biased independently of the the anode cage.

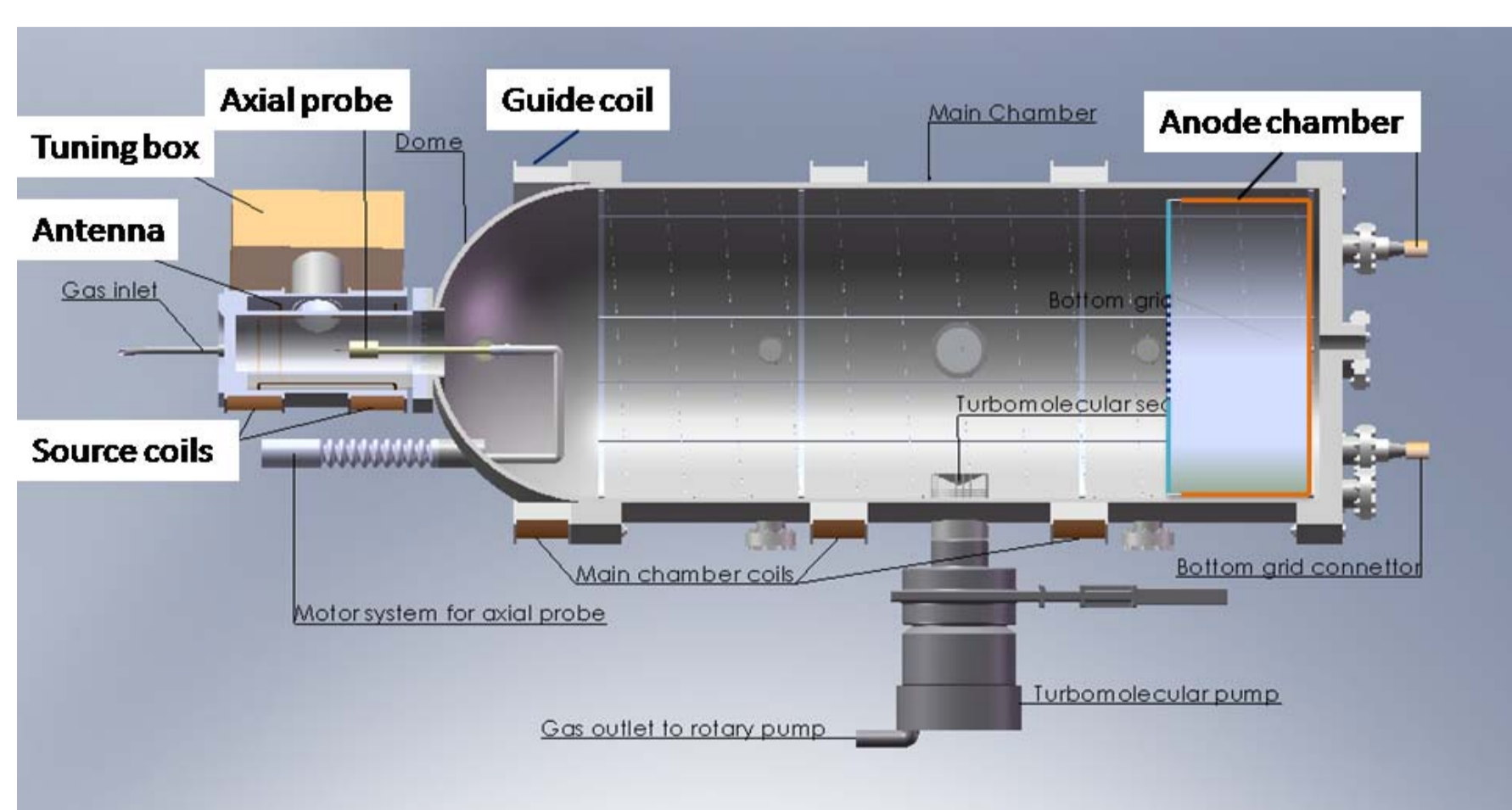


Figure 1. Outline of plasma chamber with interior and antenna system.

Magnetic field

Two (source) coils of 370 windings, diameter 24 cm, and width 10 cm each , are placed 10 cm apart on formers outside the antenna system. One more coil (the guiding coil) of 66 cm diameter is placed 28 cm downstream from the end of the 2nd source coil. It has 240 windings of 2 mm wire, and is 7 cm wide. The resulting on-axis magnetic field for some typical coil currents is shown below.

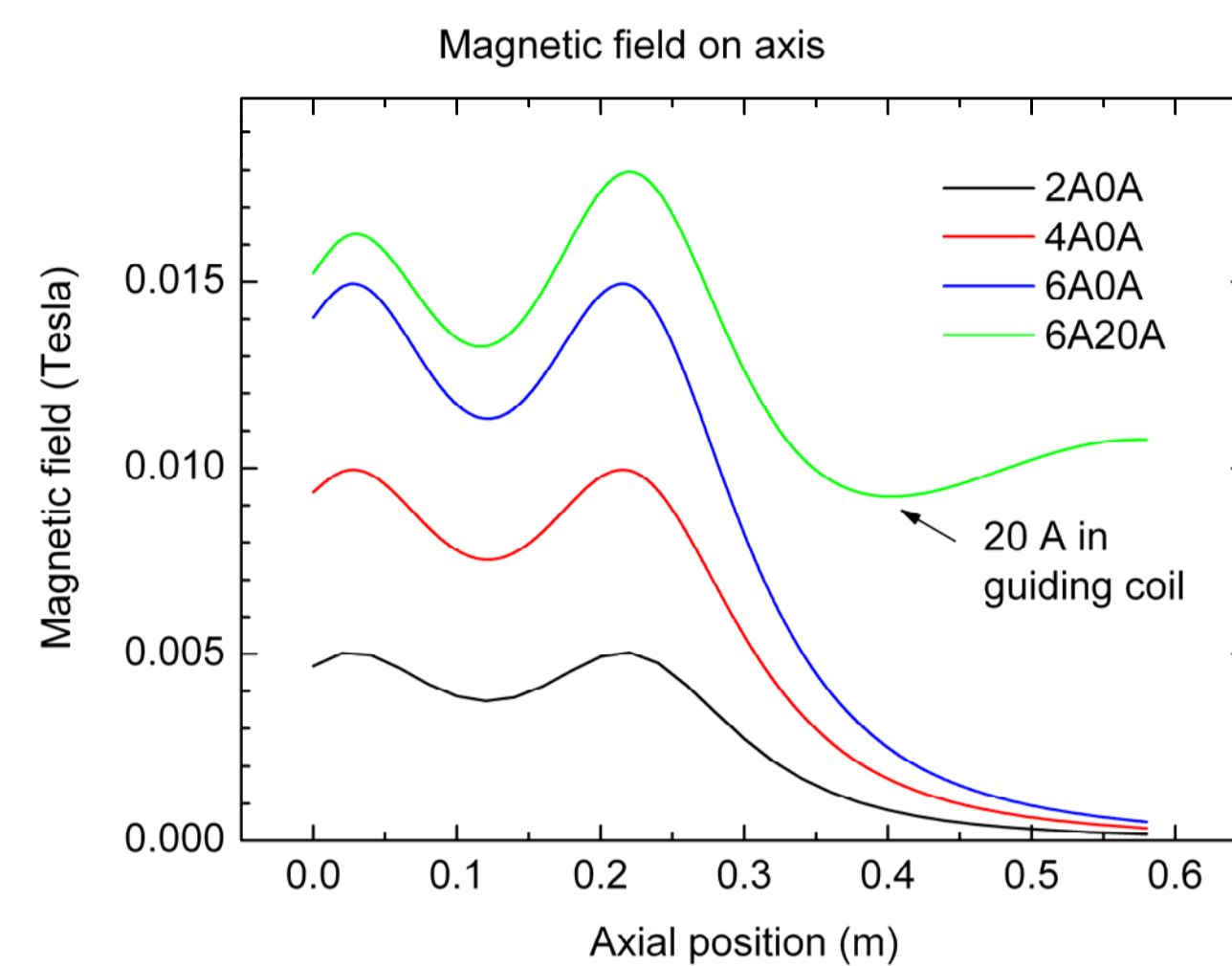


Figure 2. Axial magnetic field for three different currents in source coils with zero guide coil current and one example with source + guide coil current combined.

Plasma production

RF plasma production.

An RF source with max. 5 kW power fed to a saddle antenna (Boswell type) mounted outside a 160 mm diameter and 30 cm long pyrex tube produces an inductively coupled plasma similar to that of the Chi Kung device at ANU [1]. Fig. 3 a) shows the antenna and tuning box mounted on the 200 mm flange, with placement of probes shown, and Fig. 3 b) shows the electrical π -circuit of the RF and tuning systems. Here, L_a is the inductance of the antenna, R_{pl} is the resistance of the antenna, and C_L and C_T are variable load and tuning capacitances.

Filament plasma production.

In addition, 64 10 cm long tungsten filaments are mounted in parallel along the walls of the main chamber, and in the anode cage another 45 filaments are mounted. These can be biased negatively to the walls in the main chamber and anode cage respectively, and, when heated, can independently produce a plasma the main chamber and in the anode chamber. By biasing the anode chamber positively with respect to the main chamber, an ion beam into the main chamber can be formed.

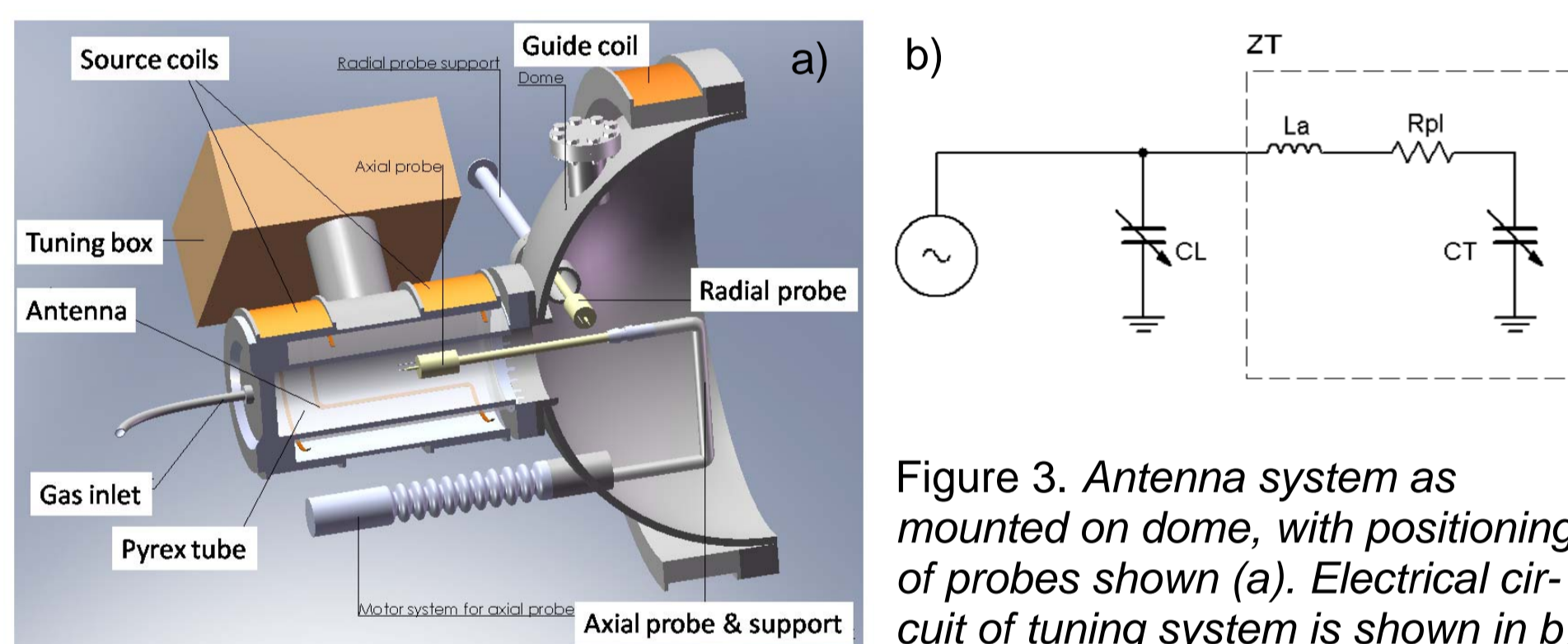


Figure 3. Antenna system as mounted on dome, with positioning of probes shown (a). Electrical circuit of tuning system is shown in b), with C_L variable from 85 to 2000 pF, and C_T from 50 to 500 pF.

Diagnostics

RF compensated probe.

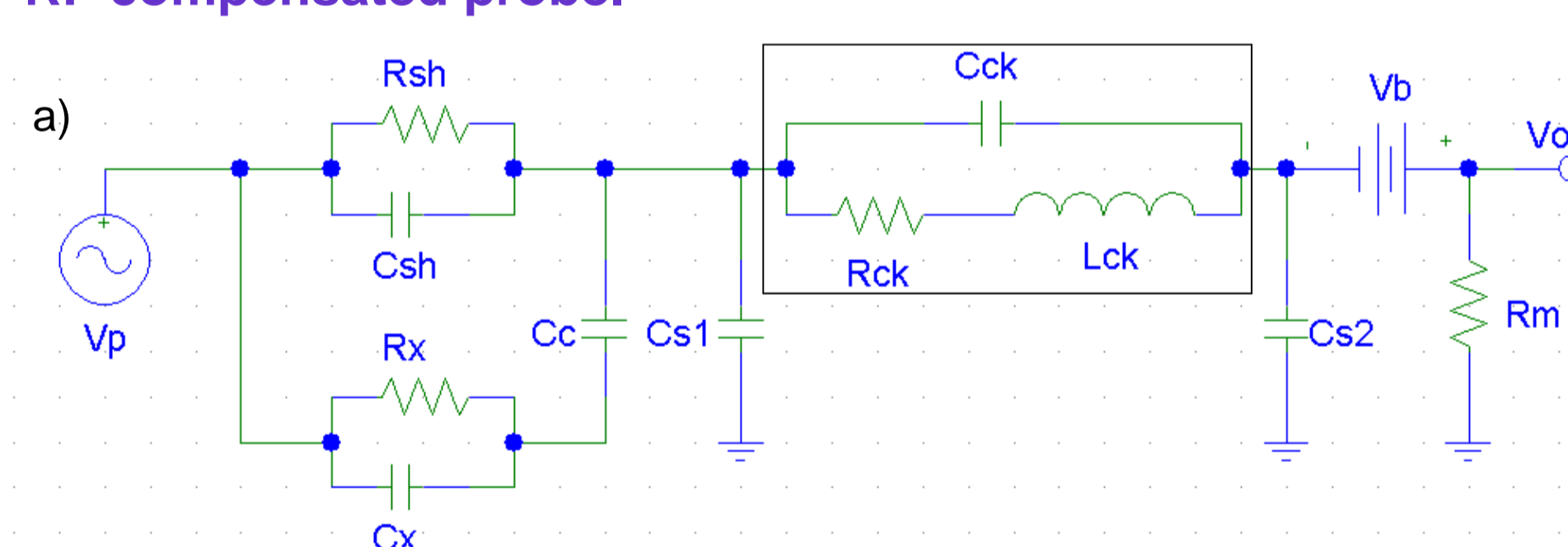


Figure 4. The probe equivalent circuitry for the RF compensated probe (a), where the components in the rectangle is the compensating circuitry; the inductance L_{ck} is $10 \mu\text{H}$, the resistor R_{ck} is small and not mounted, and the trimmer capacitor C_{ck} can be adjusted from 10 to 20 pF. A sketch of the probe, having one additional electrode for coupling to the plasma potential is shown in b), and the frequency characteristic of the filter is shown in c). Most of the measurements were carried out with this probe.

Double probe.

Double probe diagnostics was used for comparison of densities and temperature. The circuit is as used by Watts [e. g. 3] shown in Fig. 5, and the probe was a shielded double tipped Langmuir probe, with 5 mm long probe tips 3 mm apart.

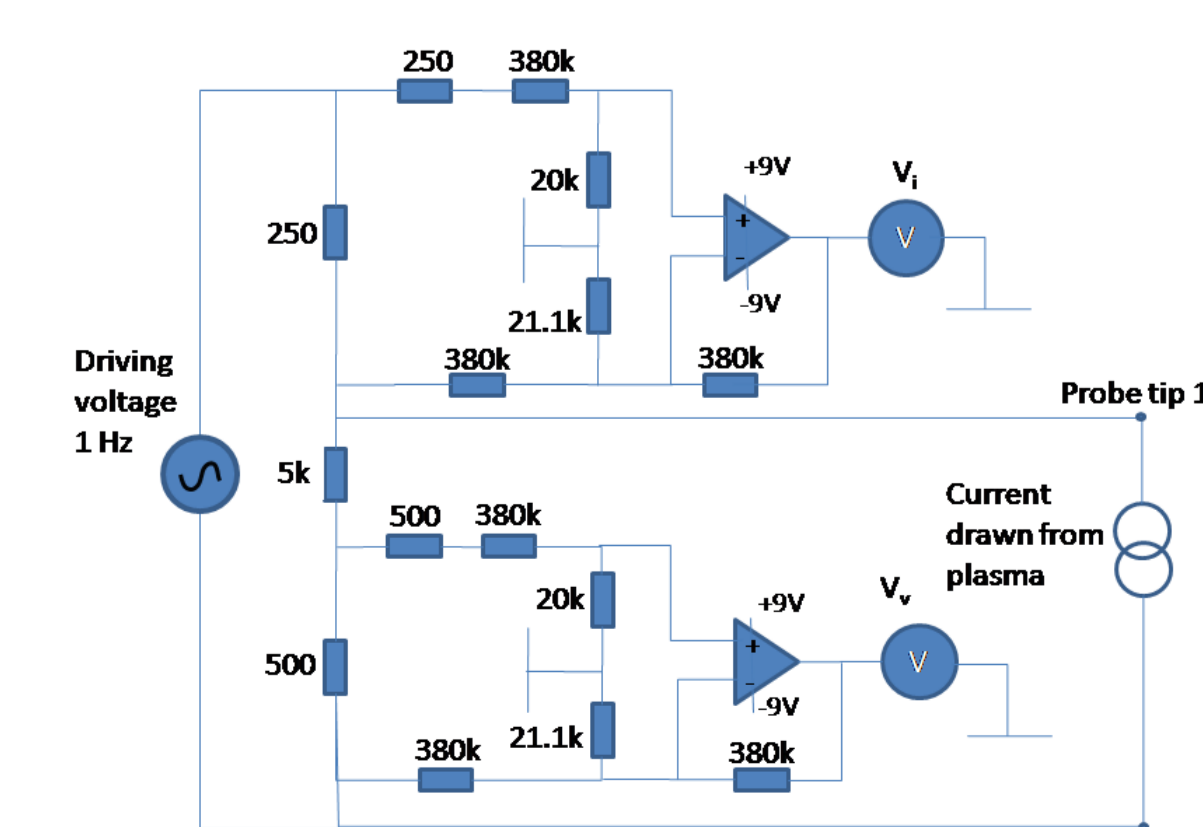


Figure 5. Schematics of double probe circuitry.

Plasma characterization

Comparison compensated Langmuir probe and double probe

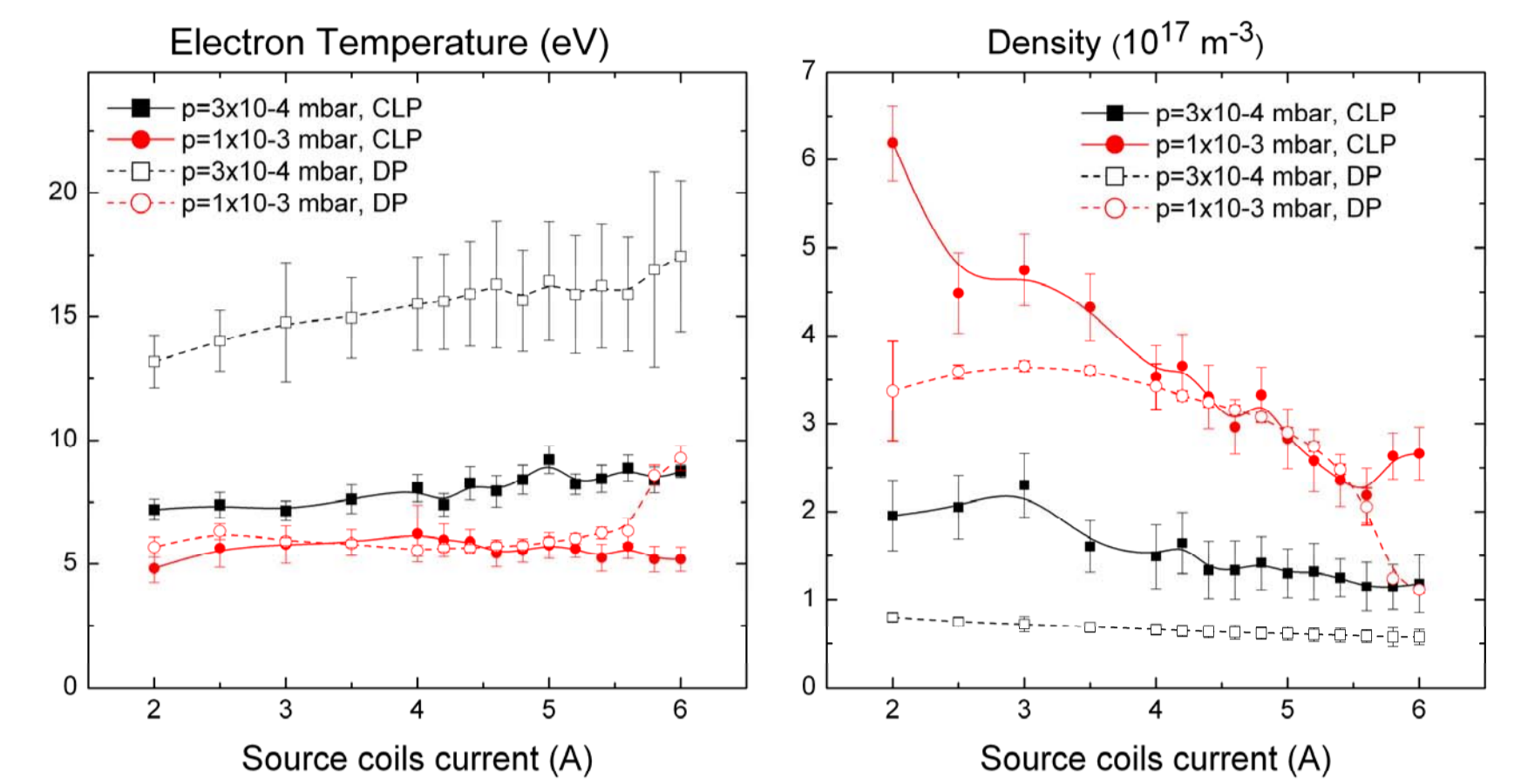


Figure 6. Electron temperature (a) and density (b) variation with source magnetic field at source entrance ($z=21$ cm), for compensated Langmuir probe (CLP, filled symbols) and double probe (DP, open symbols), and high (red) and low (black) pressures. DP data was taken with 900 Watt RF power, and CLP data was obtained with 600 Watt RF power.

The temperatures are similar at higher pressures, but the temperatures from DP probe is much larger at low pressure, partially due to a very weak signal at this pressure, but if a beam is present, the double probe is likely to pick up the high-energy tail of electrons more readily than in the LP measurements.

Axial scans with RF-compensated probe. RF power = 600 W

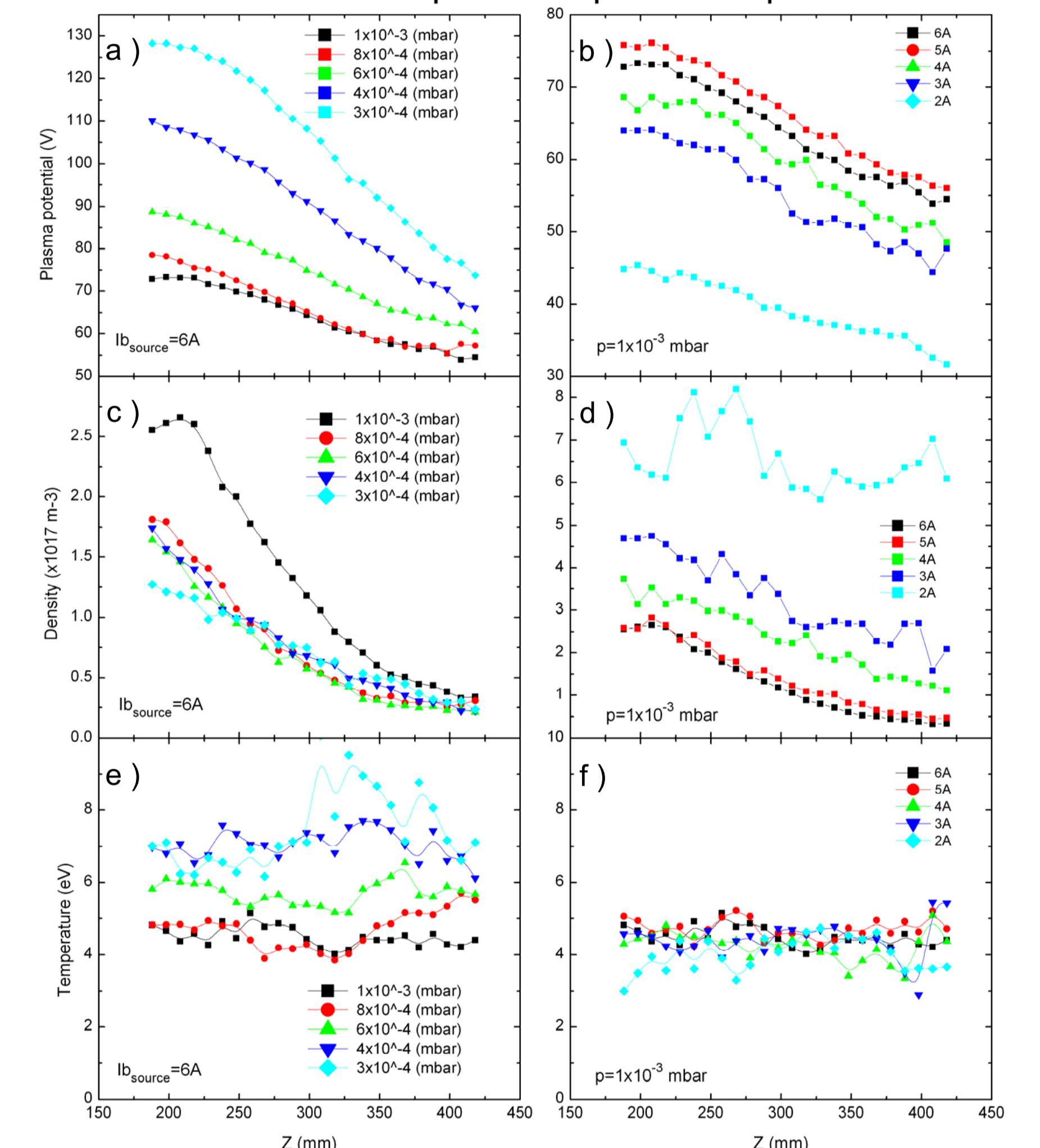


Figure 7. Axial scan of plasma potential (a, b), density (c, d), and temperature (e, f) for a set of different pressures (a, c, e) and magnetic fields (b, d, f).

Potential drop at the lowest pressure indicates an energy increase for the ions of about 20 eV between 22 and 40 cm, while area expansion alone [3] should give an upper energy limit due to area expansion (a factor 5) of about $3Te \sim 3 \times 7eV$, ie. similar to the result calculated from V_p only. Density at highest pressure and lowest magnetic field is significantly larger than the other densities, and the electron temperature is constant throughout the axial scan, although some rise in T_e at the lowest pressure may be seen at the source exit @30 cm.

Results with guide coil

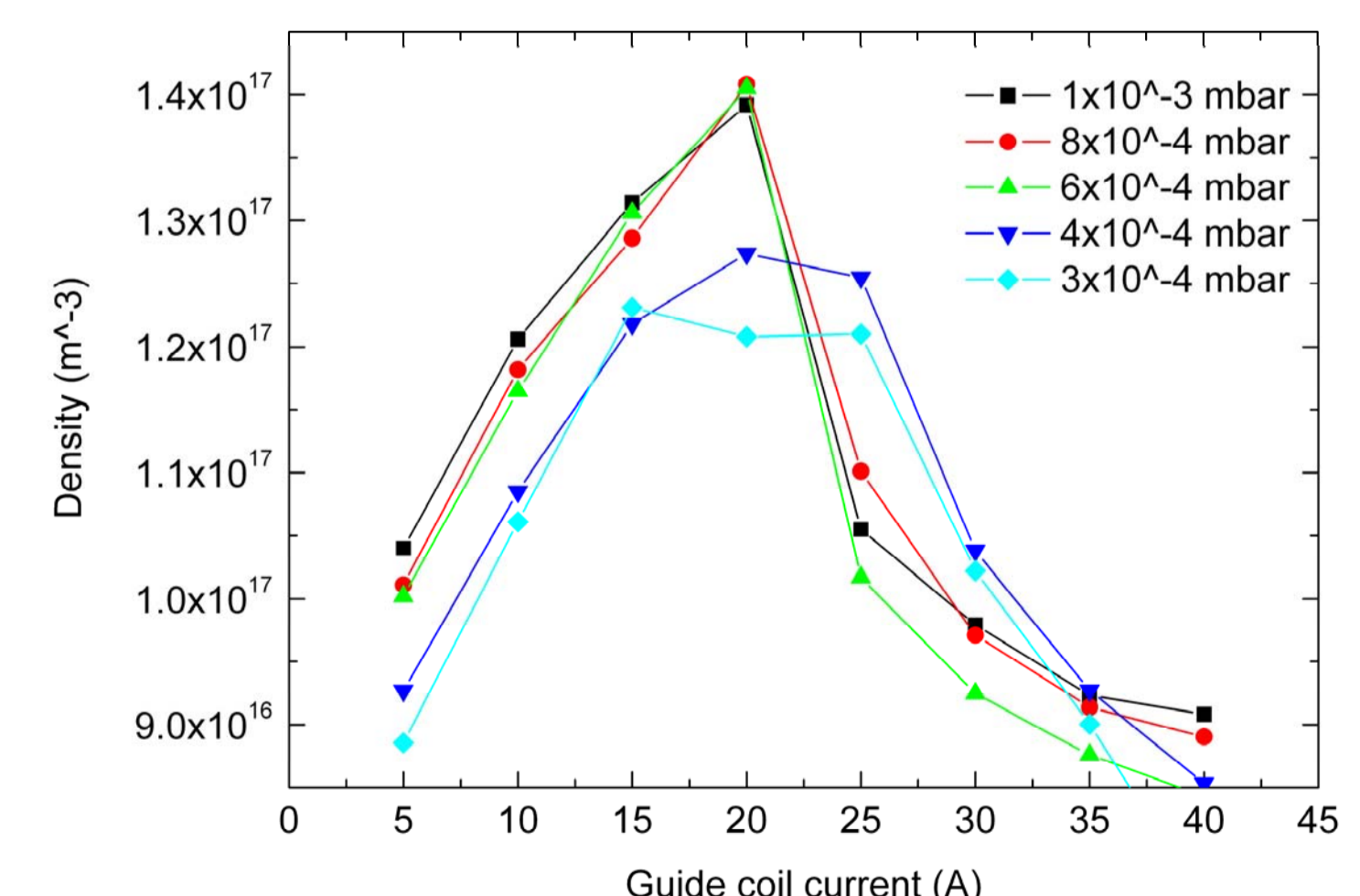


Figure 8. Variation of density 43 cm from front end of source, as a function of current in the guide coil, at five different pressures.

It is apparent from Fig. 8 that when the guiding magnetic field is increasing, the density increase with current towards a maximum > two times the density with source field current only at 6 A (ref. Fig 7c). Loss of confinement at higher guide coil fields is possibly due to the magnetic field mirroring effect as the magnetic field at the guiding coil is increasing towards values similar to those at the source. However, further modelling needs to be done in order to explain this feature properly.

Acknowledgements

The device was made possible thanks to expert help from the technical staff at Dep. Physics; Inge Strømmessen, Kjell-Arne Willumstad, and Torfinn Roaldsen, and thanks to grant provided by the University of Tromsø. We would also like to thank the PRL group at Res. School of Physical Science and Engineering, Australian National University for helpful discussions and effective manufacturing of the antenna system.

References

1. C. Charles, R. W. Boswell, and M. A. Lieberman, Phys. Plasmas, **10** (2003) 891.
2. J. Hana and C. Watts, Phys. Plasmas **8**, (2001) 4251.
3. W. M. Manheimer and R. F. Fernsler, IEEE Trans. Plasma Sci., **29**, (2001) 75